

# Sigmoidal current collector for lithium-ion battery

Meng Wang,<sup>1</sup> Anh V. Le,<sup>1</sup> Yang Shi,<sup>2</sup> Daniel J. Noelle,<sup>2</sup> Dengguo Wu,<sup>3</sup> Jiang Fan,<sup>3</sup> Weiyi Lu,<sup>4</sup> and Yu Qiao<sup>1,2,a)</sup>

<sup>1</sup>Department of Structural Engineering, University of California-San Diego, La Jolla, California 92093-0085, USA

<sup>2</sup>Program of Materials Science and Engineering, University of California-San Diego, La Jolla, California 92093, USA

<sup>3</sup>American Lithium Energy Corporation, Carlsbad, California 92008, USA

<sup>4</sup>Department of Civil and Environmental Engineering, Michigan State University, East Lansing, Michigan 48824, USA

(Received 28 October 2016; accepted 21 December 2016; published online 4 January 2017)

In the current study, we investigated sigmoidal current collector in lithium-ion battery (LIB). Traditionally, the active material in an LIB electrode is coated on a flat current collector. By rendering the current collector sigmoidal-shaped, cracking and debonding of active material layer could be promoted, which would considerably increase the internal impedance, as the LIB is mechanically abused, beneficial to thermal-runaway mitigation. The energy absorption capacity is also improved, enabling multifunctional LIB cell design. This technique has important relevance to large-sized LIB systems, for which cell robustness and fire safety are prioritized. Published by AIP Publishing. [<http://dx.doi.org/10.1063/1.4973585>]

## I. INTRODUCTION

Lithium-ion battery (LIB) has been widely applied in a wide variety of areas, such as personal electronics, electric vehicles, etc.<sup>1</sup> Recently, to promote “greener” and more efficient energy use, large-scale energy storage systems are being intensively studied [e.g., Ref. 2].

At the cell level, LIB has a specific energy around 150–250 W·h/kg and a low specific cost about \$200–\$300/kW·h, both of which are superior to acid batteries, pseudo-supercapacitors, and other options.<sup>3</sup> However, there are a number of issues that must be solved before this technique can be more broadly employed in the industry. Much research has been conducted to further increase the specific energy and to reduce the specific cost [e.g., Ref. 4]. Important “secondary” hurdles of LIB include battery safety and robustness, which will be the focus of the current investigation.

The overall electrochemical process in LIB is exothermic.<sup>5</sup> Under regular working condition, the generated heat of an LIB can be offset by the heat transfer from internal components to cell case.<sup>6</sup> In a small LIB cell, as the surface-to-volume ratio is large, the temperature change is often trivial. Even in a large-sized system, with appropriate battery thermal management system (BTMS) and battery management system (BMS), the cell temperature variation can be controlled within 1 °C. However, when an accident takes place and the battery cell is damaged, internal short circuits could be formed. In an LIB, the cathode and the anode are typically in thin film form, sandwiched with a membrane separator. The membrane separator must be highly porous and as thin as possible to optimize the ion conductivity.<sup>7</sup> If the battery cell is abused mechanically, the membrane separator can rupture and, consequently,

the cathode and the anode are in direct contact, leading to uncontrolled discharge. The local temperature can rise up to 100–120 °C in a few seconds, which triggers a series of aggressive exothermic electrochemical and chemical reactions. The reactions speed up as the temperature further increases, resulting in thermal runaway.<sup>8</sup> Moreover, the electrolytes contain highly flammable organic solvents,<sup>9</sup> which may undergo combustion or even explosion.

The concern of system robustness and fire safety continuously promotes the study on thermal-runaway mitigation.<sup>10</sup> Due to the high energy density of LIB, direct electrochemical approaches may worsen the situation. Over the years, people investigated a few indirect methods, all of which were aimed at reducing the internal short circuit current (ISCC). For instance, White *et al.*<sup>11</sup> investigated membrane separators of low melting points. As the membrane melts, it can suppress ion conduction in the electrolyte. For another example, positive thermal coefficient (PTC) additives can be mixed with the active materials.<sup>12</sup> The resistivity of PTC additives drastically rises when the local temperature approaches 110–135 °C and, therefore, the overall internal impedance increases. These mechanisms are thermally triggered, inefficient in severe shorting caused by intense mechanical abuse. To address mechanically induced thermal runaway, we investigated mechanically triggered thermal-runaway mitigation methods, e.g., by adding damage homogenizers (DHs)<sup>13</sup> or thermal-runaway retardants (TRRs)<sup>14</sup> in LIB cells. The DH additives could be microparticles of carbon black (CB) or carbon nanotubes.<sup>15,16</sup> When the battery cell was deformed, DH promoted widespread cracking and voiding in active material layers, which raised electric resistivity and lowered ISCC. With ~1 wt. % DH additives, the generated heat of a impacted LIB cell could be decreased by ~40%. While this result was interesting, the rate of temperature increase and the peak temperature were not affected.

<sup>a)</sup>Author to whom correspondence should be addressed. Electronic mail: yqiao@ucsd.edu. Telephone: +1-858-534-3388.

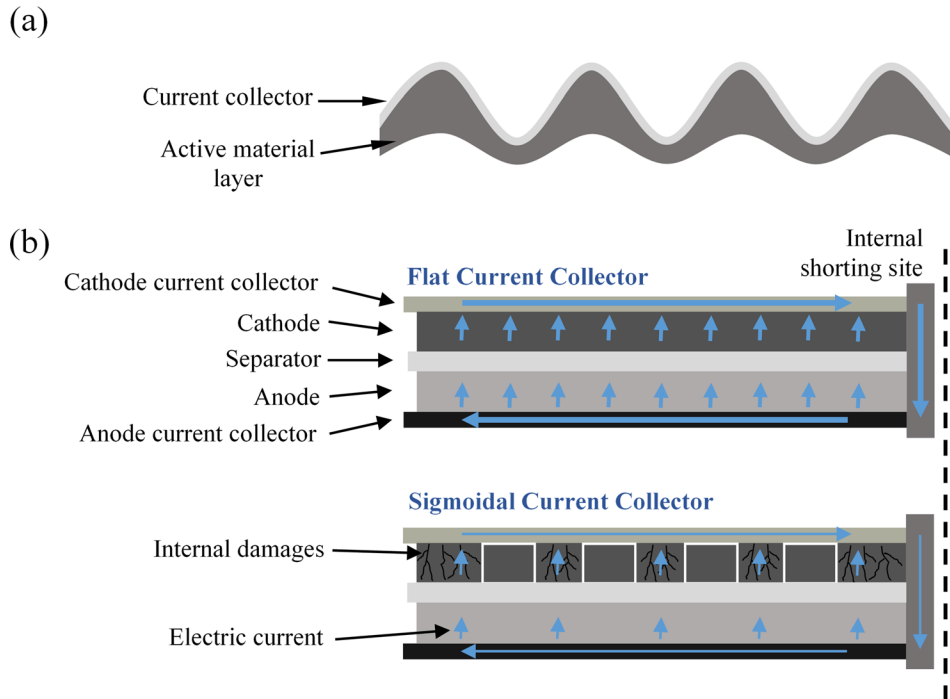


FIG. 1. (a) Schematic of sigmoidal current collector. (b) Comparison of structural changes of electrodes based on flat (top) and sigmoidal (bottom) current collectors. The blue arrows show the internal short circuit current.

In the current research, we show that modifying the geometry of current collector (Fig. 1(a)) could trigger cracking and debonding of active material layer during impact and, thus, can increase the internal impedance and limit ISCC (Fig. 1(b)). The non-planar configuration also improves the energy-absorption capability of the LIB cell, which may enable multifunctional design of battery system.

## II. EXPERIMENTS

Reference current collector was a flat 18- $\mu\text{m}$ -thick aluminum (Al) sheet. Sigmoidal current collector was created by sandwiching the flat Al sheet in between two layers of stainless steel mesh. The steel wire diameter was 500  $\mu\text{m}$  and the spacing was 2 mm. The steel-Al-steel stack was quasi-statically compressed at 10 MPa for 10 s using a type-5582 Instron machine. The loading plates were covered by 1-mm-thick

polyurethane layers. A modified current collector is shown in Fig. 2(a).

Cathode active material was prepared by blending 9.3 g of Toda America NMC-04ST, 3 wt. % Timcal carbon black (CB), and 4 wt. % Sigma-Aldrich 182702 polyvinylidene fluoride (PVDF) in a mortar for 30 min, followed by an addition of 4 ml N-methyl-pyrrolidone (NMP; Product No. 328634, Sigma-Aldrich). The active material of electrode was R $\bar{3}m$  polycrystalline  $\text{LiNi}_{0.5}\text{Mn}_{0.3}\text{Co}_{0.2}\text{O}_2$  (NMC532).<sup>17</sup> The slurry was mixed by a sonicator (Model Q55, Qsonica) for 30 min at the power level of 70%, coated on Al current collector using a film applicator (EQ-Se-KTQ-100, MTI), with the initial thickness of  $\sim 300$   $\mu\text{m}$ . The electrode was dried under vacuum at 70  $^{\circ}\text{C}$  for 24 h. The final thickness of the composite electrode layer was around 140  $\mu\text{m}$ .

Impact tests were performed on the current collectors coated by cathode active material. The coated current collector was cut into 14.3-mm-diameter circular pieces. Before

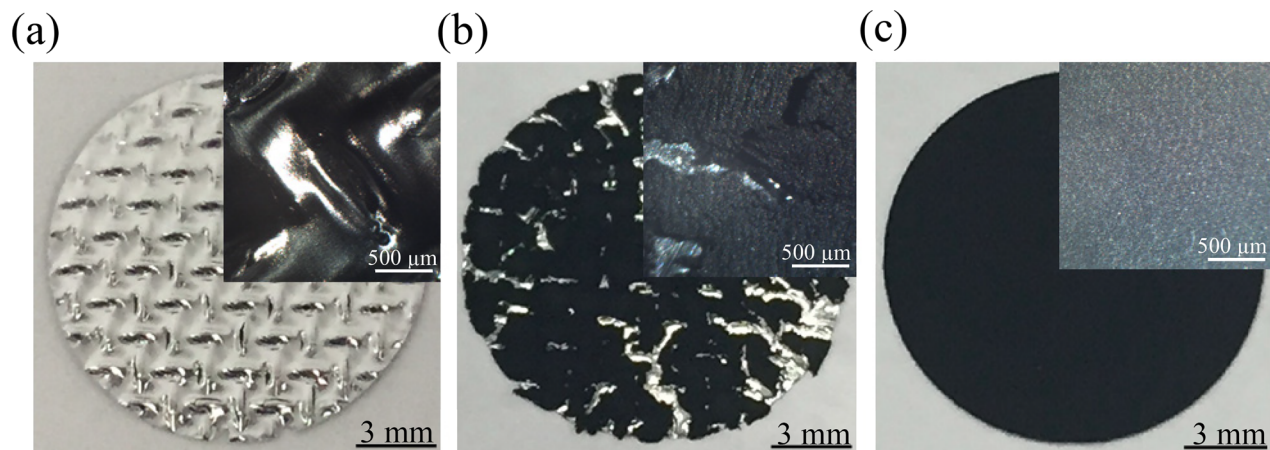


FIG. 2. (a) A modified current collector. (b) An impacted electrode based on modified current collector. (c) An impacted electrode based on reference current collector. The insets show microscopy taken by an Omana optical microscope.

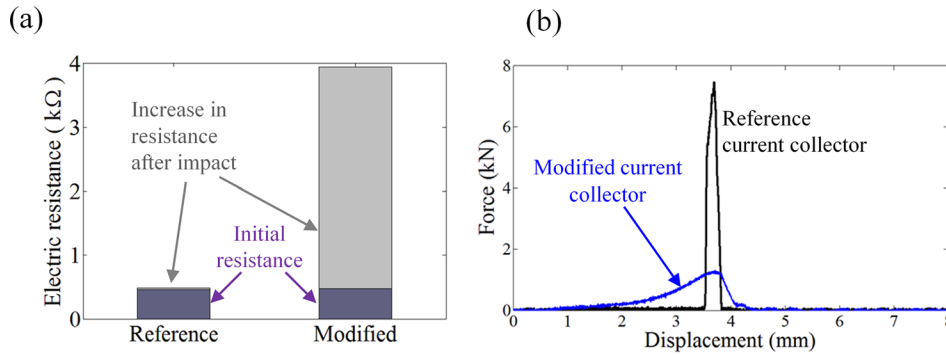


FIG. 3. (a) Increase in electric resistance of modified and reference current collectors after impact. (b) Comparison of force-displacement curves of modified and reference current collectors.

test, 100  $\mu$ l BASF electrolyte (1 M LiPF<sub>6</sub> in 1:1 EC-EMC) was dropped onto the NMC532 layer, and the sample was immediately impacted by an Instron Ceast 9350 drop tower, with the hammer mass of 2.77 kg and the impact velocity of 0.85 m/s. Figures 2(b) and 2(c) show the modified and the reference electrode layers. The surface electric resistance of the sample was measured by a BK precision multimeter before and after impact, across two probes 5 mm away from each other (Fig. 3(a)).

Impact tests were also carried out on multiple layers of reference and sigmoidal current collectors. The current collectors were sized to 20 mm  $\times$  20 mm square and formed a 10-layer stack. The layer stack was placed on a 304 stainless steel substrate and impacted by a flat steel hammer dropped by the Instron Ceast 9350 machine, with the hammer mass of 2.77 kg and the impact velocity of 1 m/s. Figure 3(b) shows typical impact profiles as a function of the hammer displacement.

Reference and sigmoidal LIB pouch cells were produced by using the same cathode and electrolyte materials. The anodes were made from graphite, CB, and PVDF, with the mass ratio of 93:1:6. The width, length, and thickness of the pouch cell were 74.6 mm, 101.3 mm, and 3.74 mm, respectively. During the last step of cell packaging, the cell was vacuum-compressed on a set of parallel 200-mm-diameter steel bars, leading to the sigmoidal configuration shown in Fig. 4(a). The magnitude and the wavelength were 8.4 mm and 101.3 mm, respectively. Reference pouch cells were compressed by planar steel plates.

Quasistatic compression was conducted on the sigmoidal pouch cells using an Instron 5582 machine. The pouch cell was confined by a 10-mm-thick U-shaped aluminum channel. The width, length, and height of the channel were 20 mm, 80 mm, and 100 mm, respectively, as illustrated in

Fig. 4(b). The load cell block had the same dimension as the inner channel so that it could be self-guided. The open circuit voltage (OCV) of each cell was measured by a BK precision multimeter before and after compression. The testing result is shown in Fig. 5(a). Before compression, the pouch cells were cycled from 3.0 V to 4.2 V under ambient condition at the rate of 0.3 C for 400 cycles. The initial capacity of each pouch cell was around 2.1 A h. Typical cycling performance is shown in Fig. 5(b).

### III. DISCUSSION

There is little debonding or cracking in an impacted reference electrode. Upon the dynamic loading, the compressive stresses are nearly uniformly distributed, and no evident damages are induced. Upon the same impact loading, a modified current collector demonstrates widespread debonding and cracking. Unlike the reference current collector, a modified current collector contains a number of stress concentration sites, and the tilted sections promote shearing and smearing.<sup>18</sup> The stress concentration factor may be assessed as:  $(1 + 2\sqrt{a/\rho}) \approx 3.2$ , where  $a \approx 300 \mu\text{m}$  and  $\rho \approx 250 \mu\text{m}$  are the characteristic size and the radius of curvature, respectively. The stresses at the crests and along the edges of the surface features are triaxial, so that cracking and debonding are pronounced. As the active material layer debonds from the current collector, the overall electric resistance will increase significantly. Before impact, the initial resistances of the electrodes based on reference and modified current collectors are similar, as they should, since the configuration of substrate does not affect the electric conductivity. The resistance of the electrode on modified current collector tends to have a slightly higher resistivity, probably due to the increase in effective surface roughness. As the electrode is impacted,

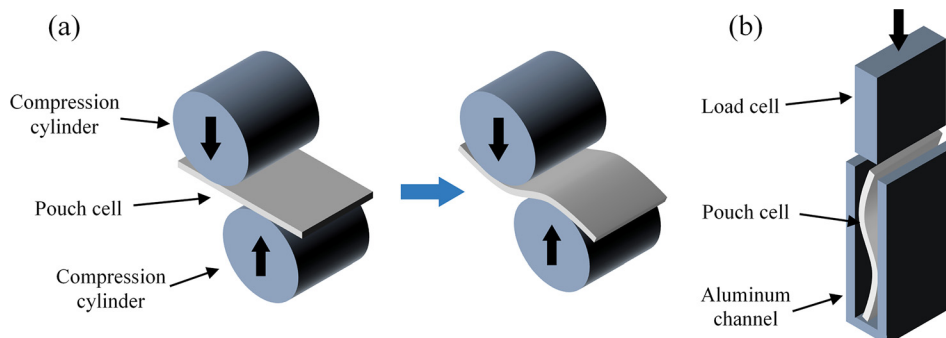


FIG. 4. (a) Setup for sigmoidal battery cell processing. (b) Quasi-static compression experimental setup.



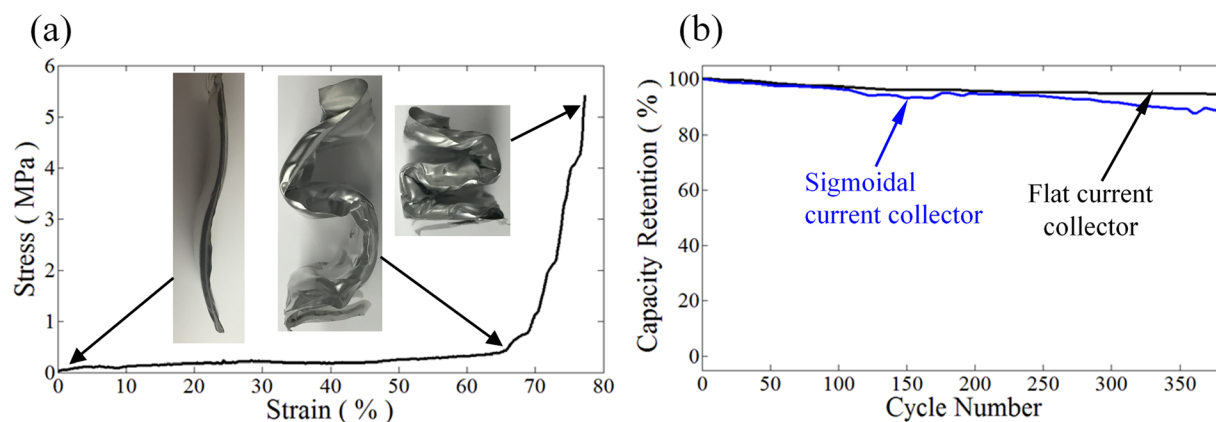


FIG. 5. (a) Mechanical response of a sigmoidal battery cell; the initial cell length is 101.3 mm (excluding the tabs). (b) Comparison of the cycling performance of sigmoidal and reference battery cells.

with a reference current collector, the resistance increases by 5%–10%. The slight increase in resistance may be caused by the loss of electrolyte. For the electrode based on modified current collector, the impact loading drastically raises the resistance by nearly an order of magnitude, associated with the evident breakage of the PVDF bonds among NMC532 particles and at the interface of active material layer and current collector. More than 50% of the NMC532 layer is separated from the Al sheet, compared to 0%–4% in reference electrodes.

In an LIB system, when a battery cell is impacted, the cell case can deform, which in turn compresses the electrodes and the membrane separator. The membrane separator has a small thickness around 10–20  $\mu\text{m}$  and a low strength around a few MPa in transverse direction<sup>19</sup> and can be quite easily ruptured. As the cathode and the anode are in contact, a large ISCC will be generated, which could rapidly trigger thermal runaway if the system does not have an appropriate safety mechanism. The impact test result of modified current collector demonstrates that, upon impact, a dense microcrack network is formed inside the active material layer, in addition to a number of broad interface cracks between the active material and the current collector. Consequently, the internal impedance,  $R$ , considerably rises. According to Ohm's law, heat generation rate may be assessed as  $q = U^2/R$ , where  $U$  is the electric potential different between cathode and anode and  $R$  is the effective impedance. When  $R$  raises by 8–9 times as measured in our experiment (Fig. 3(a)),  $q$  would be reduced to only  $\sim 12\%$  of the reference value, lower than the capacity of heat transfer.<sup>14</sup> Under this condition, the temperature increase would be much lowered.

The modified current collector also enhances the energy absorption performance of the electrode when it is impacted. In Fig. 3(b), it can be seen that, as the modified and the reference current collectors are subjected to similar impact loadings, the damping effect of the former is more evident. With the peak impact pressure of  $\sim 3$  MPa, the modified current collector undergoes plastic deformation through buckling and bending. In comparison, the reference current collector leads to a peak impact pressure  $\sim 12$  MPa, about 4 times higher. This pressure is much lower than the yield strength of aluminum and, therefore, the flat current collector only

undergoes elastic deformation, offering little protectiveness. The total absorbed energy of the electrode with modified current collector can be calculated as  $W = \int F du$ , where  $F$  is the impact force and  $u$  is the displacement. The calculated  $W$  is 1.8 J,  $\sim 90\%$  of the total impact energy of the drop hammer ( $\sim 2$  J). The absorbed energy density per unit volume is  $\sim 900$  J/l. The volume of a large-scale LIB system, e.g., the battery pack in an electric vehicle, is on the scale of 0.2  $\text{m}^3$ ,<sup>18</sup> suggesting an energy-absorption capacity on the scale of 180 kJ, equivalent to the kinetic energy of a 2-ton vehicle at the speed of  $\sim 30$  MPH.

Quasi-static compression test on sigmoidal pouch cells demonstrates its remarkable deformability, with a maximum strain of  $\sim 75\%$  and the peak pressure of  $\sim 5$  MPa (Fig. 5(a)). Before and after compression, the cell voltage was measured, respectively, as 3.58 V and 3.57 V, nearly the same. That is, the sigmoidal pouch cells may provide additional energy absorption capability without triggering internal short circuit. They can serve as not only critical energy storage units but also non-critical structural elements in an electric vehicle.

The current collector shape does not influence the battery chemistry. In fact, it tends to improve the bonding of NMC532 layer on current collector, as the effective surface area of current collector increases. Figure 5(b) suggests that the charge-discharge capacities of battery cells based on reference and sigmoidal current collectors are similar in the first 250 cycles. After 250 cycles, the sigmoidal current collector results in a faster degradation rate, probably due to the repeated swelling of active materials amplified by the stress-concentrating structure.

#### IV. CONCLUSION

To summarize, as the current collector of lithium-ion battery (LIB) is sigmoidal, the stress concentration promotes widespread cracking and debonding as the LIB cell is impacted. Consequently, the electrode resistivity increases substantially by nearly an order of magnitude, which can help mitigate thermal runaway. Moreover, the sigmoidal configuration leads to an enhanced energy absorption capacity, which can enable multifunctional design of LIB packs: that is, LIB packs can be employed as load-carrying

components, so as to reduce the overall system weight and cost. The electrochemical performance of LIB based on the sigmoidal current collector is similar to that of reference LIB in the first 250 charge-discharge cycles and degrades faster afterwards.

## ACKNOWLEDGMENTS

This research is supported by the Advanced Research Projects Agency-Energy (ARPA-E) under Grant No. DE-AR0000396, for which we are grateful to Dr. Ping Liu, Dr. John Lemmon, Dr. Grigori Soloveichik, Dr. Chris Atkinson, and Dr. Dawson Cagle.

- <sup>1</sup>V. Etacheri, R. Marom, R. Elazari, G. Salitra, and D. Aurbach, "Challenges in the development of advanced Li-ion batteries: A review," *Energy Environ. Sci.* **4**(9), 3243–3262 (2011).
- <sup>2</sup>B. Dunn, H. Kamath, and J. M. Tarascon, "Electrical energy storage for the grid: A battery of choices," *Science* **334**(6058), 928–935 (2011).
- <sup>3</sup>M. Lowe, S. Tokuoka, T. Trigg, and G. Grefi, "Lithium-ion batteries for electric vehicles: The US value chain," Center on Globalization, Governance & Competitiveness Duke University, Durham, NC, 2010.
- <sup>4</sup>J. Xu, J. Wu, L. Luo, X. Chen, H. Qin, V. Dravid, S. Mi, and C. Jia, "Co<sub>3</sub>O<sub>4</sub> nanocubes homogeneously assembled on few-layer graphene for high energy density lithium-ion batteries," *J. Power Sources* **274**, 816–822 (2015).
- <sup>5</sup>J. Zhang, H. Ge, Z. Li, and Z. Ding, "Internal heating of lithium-ion batteries using alternating current based on the heat generation model in frequency domain," *J. Power Sources* **273**, 1030–1037 (2015).
- <sup>6</sup>Z. Wang, Z. Zhang, L. Jia, and L. Yang, "Paraffin and paraffin/aluminum foam composite phase change material heat storage experimental study based on thermal management of Li-ion battery," *Appl. Therm. Eng.* **78**, 428–436 (2015).
- <sup>7</sup>X. Huang and J. Hitt, "Lithium ion battery separators: Development and performance characterization of a composite membrane," *J. Membr. Sci.* **425**, 163–168 (2013).

- <sup>8</sup>Q. Wang, P. Ping, X. Zhao, G. Chu, J. Sun, and C. Chen, "Thermal runaway caused fire and explosion of lithium ion battery," *J. Power Sources* **208**, 210–224 (2012).
- <sup>9</sup>L. Hu, Z. Zhang, and K. Amine, "Fluorinated electrolytes for Li-ion battery: An FEC-based electrolyte for high voltage LiNi<sub>0.5</sub>Mn<sub>1.5</sub>O<sub>4</sub>/graphite couple," *Electrochem. Commun.* **35**, 76–79 (2013).
- <sup>10</sup>M. M. Thackeray, C. Wolverton, and E. D. Isaacs, "Electrical energy storage for transportation—Approaching the limits of, and going beyond, lithium-ion batteries," *Energy Environ. Sci.* **5**(7), 7854–7863 (2012).
- <sup>11</sup>M. Baginska, B. J. Blaiszik, R. J. Merriman, N. R. Sottos, J. S. Moore, and S. R. White, "Autonomic shutdown of lithium-ion batteries using thermoresponsive microspheres," *Adv. Energy Mater.* **2**(5), 583–590 (2012).
- <sup>12</sup>P. G. Balakrishnan, R. Ramesh, and T. P. Kumar, "Safety mechanisms in lithium-ion batteries," *J. Power Sources* **155**(2), 401–414 (2006).
- <sup>13</sup>A. V. Le, M. Wang, Y. Shi, D. J. Noelle, and Y. Qiao, "Heat generation of mechanically abused lithium-ion batteries modified by carbon black micro-particulates," *J. Phys. D: Appl. Phys.* **48**(38), 385501 (2015).
- <sup>14</sup>Y. Shi, D. J. Noelle, M. Wang, A. V. Le, H. Yoon, M. Zhang, Y. S. Meng, and Y. Qiao, "Exothermic behaviors of mechanically abused lithium-ion batteries with dibenzylamine," *J. Power Sources* **326**, 514–521 (2016).
- <sup>15</sup>A. V. Le, M. Wang, Y. Shi, D. Noelle, Y. Qiao, and W. Lu, "Effects of additional multiwall carbon nanotubes on impact behaviors of LiNi<sub>0.5</sub>Mn<sub>0.3</sub>Co<sub>0.2</sub>O<sub>2</sub> battery electrodes," *J. Appl. Phys.* **118**(8), 085312 (2015).
- <sup>16</sup>M. Wang, A. V. Le, Y. Shi, D. Noelle, H. Yoon, M. Zhang, Y. S. Meng, and Y. Qiao, "Effects of angular fillers on thermal runaway of lithium-ion battery," *J. Mater. Sci. Technol.* (in press).
- <sup>17</sup>J. Z. Kong, C. Ren, G. A. Tai, X. Zhang, A. D. Li, D. Wu, H. Li, and F. Zhou, "Ultrathin ZnO coating for improved electrochemical performance of LiNi<sub>0.5</sub>Co<sub>0.2</sub>Mn<sub>0.3</sub>O<sub>2</sub> cathode material," *J. Power Sources* **266**, 433–439 (2014).
- <sup>18</sup>J. T. Warner, *The Handbook of Lithium-Ion Battery Pack Design: Chemistry, Components, Types and Terminology* (Elsevier, 2015).
- <sup>19</sup>A. Sheidaei, X. Xiao, X. Huang, and J. Hitt, "Mechanical behavior of a battery separator in electrolyte solutions," *J. Power Sources* **196**(20), 8728–8734 (2011).